The Journal of Navigation (2021), **74**:3 673–697
doi:10.1017/S037346332000065X

RESEARCH ARTICLE

Ship domain model for ships with restricted manoeuvrability in busy waters

Wei Pan,[1] Xin-lian Xie,[1]* Tian-tian Bao,[2] and Meng Li[1]

[1] Integrated Transport Institute, Dalian Maritime University, Dalian 116026, China.
[2] Faculty of Maritime and Transportation, Ningbo University, Ningbo 315211, China.
*Corresponding author. E-mail: xxlian@dlmu.edu.cn

Received: 16 March 2020; **Accepted:** 30 November 2020; **First published online:** 22 January 2021

Keywords: ship domain, ship collision, AIS, safety

Abstract

Ship domain is an important theory in ship collision avoidance and an effective collision detection method. First, several classical ship domain models are used in experiments. The results show that the alarm rate is too high in busy waters, leading to greatly reduced practicality of the model. Potential collision risk cannot be detected effectively, especially for a ship with restricted manoeuvrability, which is usually regarded as an overtaken ship due to its navigation characteristics. Therefore, it is necessary to fully consider the interference of other ships to ships with limited manoeuvrability in an encounter situation. A novel ship domain model for ships with restricted manoeuvrability in busy waters is proposed. Considering the navigation characteristics of a ship with restricted manoeuvrability and the influence of the ship–ship effect, an algorithm to determine the boundary of the ship domain model is given by force and moment equations. AIS trajectory data of the North Channel of the Yangtze River Estuary are used to perform a comparative experiment, and four classical ship domain models are employed to perform comparative experiments. The results show that the alarm rates of the novel ship domain model are 7·608%, 15·131%, 55·785% and 7·608% lower than those of the other four classical models, and this outcome can effectively reduce the high false alarm rate produced by other models in this environment.

1. Introduction

With the rapid development of a coastal economic zone and riverside economic zone, the ship traffic volume and ship density of China's coastal waters are increasing gradually. Moreover, with the continuous development of the shipbuilding industry, ships are being built at a large scale and for high speeds. As a result, some coastal shallow waters cannot satisfy the navigation requirements of large ships. As a result, some engineering ships frequently conduct dredging operations in the channel. Currently, the collision risk between a passing cargo ship and a dredging engineering ship has increased sharply, which more seriously causes serious damage to ships, delays in project progress and immense economic losses. Therefore, detecting the collision risk between passing ships and engineering ships has great significance for safety on the oceans.

According to the Convention on the International Regulations for Preventing Collisions at Sea (COLREGS), a self-propelled trailing-suction dredger is a typical ship with restricted manoeuvrability. According to the characteristics of its operation, it is impossible for it to avoid passing ships in a timely and effective manner. Therefore, due to the engineering value and unique operation mode of a self-propelled trailing suction dredger, it is necessary to ensure the navigation safety of a ship with restricted manoeuvrability, such as a self-propelled trailing-suction dredger.

Ship domain is a concept of collision avoidance that was proposed by the Japanese scholar Fujii. The mechanism of ship domain is a two-dimensional area that surrounds a ship, which other ships must avoid, used to realise the risk identification of ship collision between a ship and other ships. Based on the investigation of previous ship domain models and the experimental analysis of part of them, it can be determined that previous ship domain models are not suitable for the application of a ship with restricted manoeuvrability in busy waters. Therefore, a novel ship domain model of a ship with restricted manoeuvrability that is suitable for busy waters is urgently needed.

To design a ship domain model for a ship with restricted manoeuvrability, the traditional ship mechanics principle is applied to analyse the boundary scale of the novel ship domain. By the investigation of AIS data in busy waters, it can be determined that self-propelled trailing-suction dredgers operate in the channel, and other ships will need a relatively short distance to complete an encounter or overtaking, which explains why classical ship domain models cannot be applied to self-propelled dredgers in busy waters. Therefore, in addition to human factors, the influence of the ship–ship effect has become the main influencing factor. In this paper, the boundary of the novel ship domain model is solved by using the ship–ship effect computational model, ship directional keeping ability computational model and ship manoeuvrability equation.

Different from classic ship domain models, the novel ship domain model proposed in this paper focuses on the situation in which a ship with restricted manoeuvrability encounters other ships in busy waters. A ship with restricted manoeuvrability cannot make way for overtaking a ship or encountering a ship. Therefore, the navigation characteristics of a ship with restricted manoeuvrability are fully considered when determining the model boundary. In addition, as the main reason that affects the navigation of ships in busy waters, the calculation of the ship–ship effect has been innovatively added to the calculation of the boundary determination of the ship domain. In the application of this novel model, the ship domain model will give a suitable model scale for the current ship combination according to their ship parameters and navigation parameters. The novel model is different from the classic fixed-scale ship domain models. Therefore, the novel model can be better applied to collision risk identification of ships with restricted manoeuvrability in busy waters.

The remainder of this paper is organised as follows: Section 2 is a brief literature review of the ship domain and relevant supporting theories. Section 3 provides the complete design of the ship domain model and the method of parameters estimation. In Section 4, the parameters estimation method is tested, and then the ship domain model is verified by experiments. The conclusions are discussed in Section 5.

2. Related work

The identification of ship collision risk has always been a popular research area in the field of navigation. Different scholars adopt different methods to solve different problems. From the perspective of the macro method, with the development of science and technology, ship collision risk identification has experienced several important stages, such as the analytical method, statistical method and intelligent method. After years of development, there are an increasing number of ways to identify ship collision risk. The methods of ship collision risk identification and assessment have been gradually investigated (Wang et al., 2017; Argüelles et al., 2019; Zhang et al., 2019; Zhao-Kun et al., 2020).

The ship domain model was first proposed by Fujii (Fujii and Tanaka, 1971). Fujii employed radar data for statistical analysis and discovered that a two-dimensional ship free area always existed around the selected ship. Via a large number of statistics, the basic dimension of the ship domain was given. In the early stage of ship domain studies, different scholars proposed different models. Goodwin proposed a new type of ship domain model that is composed of three unequal sectors via an actual investigation and simulated a collision avoidance experiment at sea (Goodwin, 1975). Tak combined the advantages of the Fujii model and Goodwin model and proposed a novel ship domain model (Van der Tak and Spaans, 1977). To facilitate practical application, Davis smoothed the boundary based on the Goodwin model and successfully obtained the circular ship domain model (Davis et al., 1980). After the observation of maritime traffic, Coldwell established a ship domain model for an encounter situation (Coldwell, 1983).

https://doi.org/10.1017/S037346332000065X Published online by Cambridge University Press

With the development of ship domain theory, the research methods of the ship domain model gradually developed into three categories: statistical model, artificial intelligence model and analytical method model. The statistical model is a common method that was employed by early scholars and is still employed in current research. Hansen obtained ship volume data on the waters near Denmark and determined the boundary dimensions of the ship domain model by performing a large number of experiments (Hansen et al., 2013). Wang and Chin performed a statistical analysis of ship traffic flow data on Singapore and the Singapore Strait, assumed the relationship between the size of the ship domain model and the ship parameters, and solved the assumed relationship coefficient by a genetic algorithm (Wang et al., 2016). Goerlandt proposed a ship domain model based on a ship's navigation state and ice zone state in the research of a ship's ice zone navigation safety (Goerlandt et al., 2016).

Big data and artificial intelligence have become the main research methods in various industries, a reliance on data analysis cannot satisfy part of the research needs. Therefore, the artificial intelligence method is extensively employed in various fields. Some scholars also apply the artificial intelligence method to ship domain model research. Zhu conducted a survey of a ship crew by means of a questionnaire and trained the Back Propagation neural network model (BP neural network model) with the survey results, by which the basic situation of the ship domain was determined (Zhu et al., 2001). Pietrzykowski also employed the method of collecting ship domain knowledge to obtain training samples, trained the fuzzy neural network model, and determined the ship domain model in a narrow channel and open water area (Pietrzykowski, 2008; Pietrzykowski and Uriasz, 2009). Based on 600,000 ship encounters in 36 locations, Hörteborn analysed the determination of the ship domain model boundary scale and discussed the factors that influence the scale (Hörteborn et al., 2018).

The analytic method is another main method to determine the ship domain model. By analysing the influence of different factors on the ship domain scale, the exact boundary or algorithm can be obtained to determine the ship domain boundary scale. Zhao proposed a fuzzy ship domain by analysing the shortcomings of the classical ship domain. The model can consider the influence of different factors on ship navigation safety and then realise the identification of the ship navigation risk by changing the scale of the ship domain (Jingsong et al., 1993). Wang proposed a quaternion ship domain by an analytic method, in which the boundary is determined by the radius of the ship in four directions and boundary parameters, which considers the ship speed, ship scale and ship manoeuvrability. Based on the quaternion ship domain model, fuzzy quaternion ship domain (FQSD) and dynamic quaternion ship domain (DQSD) are proposed (Wang, 2010, 2013). Dinh proposed a quadrilateral ship domain model that considers the approach distance between two ships and proposed the concept of 'action area', which means that the second ship enters the range and the first ship needs to adopt a collision avoidance manoeuvre (Dinh and Im, 2016). Zhou proposed a new dynamic fuzzy ship domain model, which considers the relevant factors of a ship and other ships and applied the method of neural network and wavelet decomposition to analyse the factors that influence the scale of the model. (Zhou and Zheng, 2018). Zhang proposed a ship domain model with a fuzzy boundary and a large AIS data-driven method to determine the probability domain of ships (Zhang and Meng, 2019). Im proposed a potential risk ship domain (PRSD) model with a clear meaning of risk degree and simultaneously evaluated the risk of collision threat by the navigation state of surrounding ships (Im and Luong, 2019). Remzi proposed an asymmetrical ship domain model that is based on a fuzzy rule-based model for open waters and restricted waters (Fiskin et al., 2020).

In this paper, an analytical method is employed to study the domain model for a ship with restricted manoeuvrability in busy waters. According to the environmental factors and the ship's manoeuvrability factors, the proposed ship domain model should consider the ship manoeuvrability, ship–ship effect, and ships' directional ability. To quantify the impact of these factors on ships, a ship mechanics method is employed for the quantitative analysis. Some calculation concepts and models of the ship motion mathematical model will be applied to determine the novel ship domain model. In the field of numerical calculation of the ship–ship effect, Yeung applied slender body theory to study the unsteady hydrodynamic interaction of two ships moving in shallow fluid. However, the calculation of this method depends on specific ship parameters, which is difficult to achieve (Yeung, 1978). Gourlay proposed

https://doi.org/10.1017/S037346332000065X Published online by Cambridge University Press

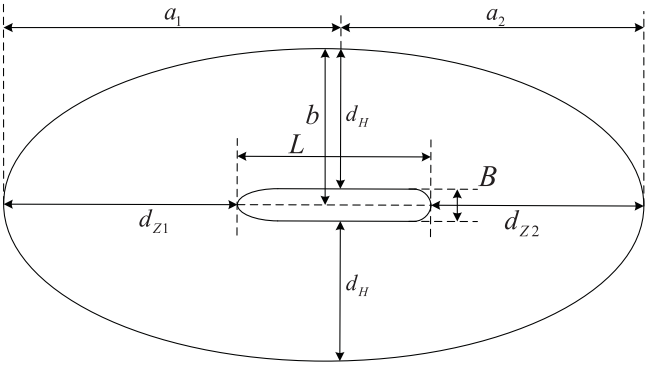

Figure 1. *Schematic of the ship domain.*

a numerical calculation method of the hydrodynamic action between two ships in the situation of encountering and overtaking and examined the response of the interaction between the ships to the ships' sinking and trim. This method requires a ship's profile data, for which popularisation in a practical application process is difficult (Gourlay, 2009). Similarly, Lataire proposed a mathematical model of the hydrodynamic effect between a large ship and a small ship when they were engaged in a lightering operation (Lataire et al., 2012). Varyani proposed ship–ship effect research results in different situations, including the calculation model of the ship–ship effect of two ships in an encounter situation, an overtaking situation, an anchoring situation and a multi-ship encounter situation (Varyani et al., 2004; Varyani and Krishnankutty, 2006). The ship parameters required by the Varyani model are easily obtained, and the model has high calculation accuracy. Therefore, this paper employs the Varyani model to carry out the mechanical calculation of the ship-ship effect.

3. Ship domain model

3.1. Method for determination of the ship domain boundary

The boundary of the ship domain determines its application effect. The spacing between two ships is generally small in busy waters. Especially in narrow waterways, the ship with restricted manoeuvrability is always the overtaken ship in an encounter situation. At this time, the overtaken ship faces collision risk from other ships on the bow, stern and side. Therefore, the ship domain boundary can be determined from two aspects: horizontal safety distance and longitudinal safety distance, which are shown in Figure 1.

The boundary of the ship domain can be described by two semi-ellipses that have the same short axis and different long axes. The significance of the parameters of Figure 1 are expressed as follows: L = ship length, B = ship breadth, d_H = transverse safety distance, d_{Z1} and d_{Z2} = longitudinal safety distance, a_1 and a_2 = long axes of two semi-ellipses, and b = short axis of the ellipse. The long axis and short axis can be expressed as Equations (1) and (2), respectively:

$$a_i = L/2 + d_{Zi} (i = 1, 2) \tag{1}$$

$$b = B/2 + d_H \tag{2}$$

3.2. Transverse safety distance determination method

According to the method for determining the ship domain boundary, the novel ship domain model uses the elliptical boundary. The short axis of the ellipse consists of the ship breadth and the transverse safety distance. The transverse safety distance between two ships, which consists of different factors, should be maintained. However, the ship–ship effect is an important factor that affects ship navigation safety in busy waters, where the density of ships is higher and the spacing between ships is smaller. Therefore,

https://doi.org/10.1017/S037346332000065X Published online by Cambridge University Press

the transverse safety distance, which considers the ship–ship effect, is taken as the transverse boundary distance of the novel ship domain model.

3.2.1. Calculation of ship–ship interaction effect

The numerical calculation of the ship–ship effect adopts the general calculation model proposed by Varyani (Varyani et al., 2004; Varyani and Krishnankutty, 2006). In a head-on situation, the coefficient of the transverse drift force = C_{Fi}, and the coefficient of the bow moment = C_{Ni}. The two coefficients can be expressed as

$$\begin{cases} C_{Fi} = -0{\cdot}47\cos(0{\cdot}86\pi t)e^{(-0{\cdot}95t^2)}(1+0{\cdot}18t) \\ \qquad \left(\dfrac{2H}{3d_m}\right)^{-2{\cdot}25}\left(\dfrac{2S_P}{L_i}\right)^{-1{\cdot}25}\left(\dfrac{L_1}{L_2}\right)^{-2{\cdot}5}\left(0{\cdot}5+\dfrac{U_2}{2U_1}\right) \\ C_{Ni} = 0{\cdot}15\cos(0{\cdot}86\pi t)e^{(-0{\cdot}95t^2)}(1+0{\cdot}18t)(t+\Delta)A(t) \\ \qquad \left(\dfrac{2H}{3d_m}\right)^{-2{\cdot}25}\left(\dfrac{2S_P}{L_i}\right)^{-1{\cdot}25}\left(\dfrac{L_1}{L_2}\right)^{-2{\cdot}5}\left(0{\cdot}5+\dfrac{U_2}{2U_1}\right) \end{cases} \tag{3}$$

In an overtaking situation, the coefficient of the transverse drift force of the overtaking ship = C_{F1}, and the coefficient of the bow moment = C_{N1}. The coefficient of the transverse drift force of the overtaken ship = C_{F2}, and the coefficient of the bow moment = C_{N2}. The expression of the four coefficients can be expressed as

$$\begin{cases} C_{F1} = -0{\cdot}11\sin(-0{\cdot}49\pi(t+0{\cdot}37))e^{(-0{\cdot}95t^2)}(1-0{\cdot}98t) \\ \qquad \left(\dfrac{2H}{3d_m}\right)^{-1{\cdot}8}\left(\dfrac{2S_P}{L_i}\right)^{-1{\cdot}0}\left(\dfrac{L_1}{L_2}\right)^{-1{\cdot}5}\left(\dfrac{3U_2}{4U_1}-0{\cdot}5\right) \\ C_{N1} = -0{\cdot}1\sin(-0{\cdot}49\pi(t+0{\cdot}07))e^{(-0{\cdot}9t^2)}(1-0{\cdot}3t)A(t) \\ \qquad \left(\dfrac{2H}{3d_m}\right)^{-1{\cdot}8}\left(\dfrac{2S_P}{L_i}\right)^{-1{\cdot}0}\left(\dfrac{L_1}{L_2}\right)^{-1{\cdot}5}\left(\dfrac{3U_2}{4U_1}-0{\cdot}5\right) \\ C_{F2} = -0{\cdot}23\cos(-0{\cdot}9\pi t)e^{(-0{\cdot}8t^2)}(1-0{\cdot}18t) \\ \qquad \left(\dfrac{2H}{3d_m}\right)^{-2{\cdot}2}\left(\dfrac{2S_P}{L_i}\right)^{-1{\cdot}3}\left(\dfrac{L_1}{L_2}\right)^{-0{\cdot}35}\left(\dfrac{3U_2}{4U_1}-0{\cdot}5\right) \\ C_{F2} = -0{\cdot}23\cos(-0{\cdot}65\pi(t+0{\cdot}05))e^{(-1{\cdot}5t^2)}(1-0{\cdot}18t)A(t) \\ \qquad \left(\dfrac{2H}{3d_m}\right)^{-2{\cdot}2}\left(\dfrac{2S_P}{L_i}\right)^{-1{\cdot}3}\left(\dfrac{L_1}{L_2}\right)^{-0{\cdot}35}\left(\dfrac{3U_2}{4U_1}-0{\cdot}5\right) \end{cases} \tag{4}$$

where t = non-dimensionalised stagger distance between two ships, which can be expressed as

$$t = \frac{2ST_{12}}{L_1+L_2} \tag{5}$$

where ST_{12} = staggered distance between two ships in the longitudinal direction, H = depth of the navigation water area, d_m = draft of the ship, S_P = transverse distance between the two ships, L_i = length of the ships and U_i = speed of the ships, where i is used to mark the number of the ship. $A(t)$ can be computed by

$$A(t) = 1 - ae^{-b(t-t_0+\Delta)^2} \tag{6}$$

https://doi.org/10.1017/S037346332000065X Published online by Cambridge University Press

The coefficients of Equation (6) can be expressed as

$$\begin{cases} a = 0{\cdot}3\dfrac{h}{d_m} + 1{\cdot}4\dfrac{S_P}{L} + 0{\cdot}3\dfrac{L_1}{L_2} + 0{\cdot}5\dfrac{U_1}{U_2} \\ b = 1{\cdot}4\dfrac{h}{d_m} + 5\dfrac{S_P}{L} + 1{\cdot}4\dfrac{L_1}{L_2} + 6\dfrac{U_1}{U_2} \\ t_0 = -0{\cdot}5\dfrac{h}{d_m} - \dfrac{S_P}{L} - 0{\cdot}5\dfrac{L_1}{L_2} - \dfrac{U_1}{U_2} \\ \Delta = -0{\cdot}1\dfrac{h}{d_m} - 0{\cdot}1\dfrac{S_P}{L} - 0{\cdot}1\dfrac{L_1}{L_2} - 0{\cdot}2\dfrac{U_1}{U_2} \end{cases} \tag{7}$$

The transverse drift force and bow moment can be expressed as

$$\begin{cases} F_{Ex} = 0{\cdot}5\rho U_1 U_2 B_1 d_{m1} C_{Fx} \\ N_{Ex} = 0{\cdot}5\rho U_1 U_2 B_1 d_{m1} L_1 C_{Nx} \end{cases} \tag{8}$$

3.2.2. Numerical calculation of ship's directional keeping capacity

A ship's directional keeping capacity is an important index to measure a ship's manoeuvrability. Directional keeping control is a kind of straight-line motion that can make a ship recover its original course in a short time with a small rudder angle. According to the hydrodynamic calculation results of the rudder by early scholars, the critical rudder angle is mostly 35°–40°, while the maximum rudder angle of most ships is approximately 35° (Curtis, 1980). Ship manoeuvrability includes small rudder angle keeping, initial turning of the middle rudder angle and large rudder angle turning. However, the specific value of the small rudder angle is not defined clearly. Combined with the ship's maximum rudder angle of 35°, the distribution of the rudder angle can be approximately determined: small rudder angle (5°–15°), middle rudder angle (20°–25°) and large rudder angle (30°–35°). Therefore, the numerical value of small rudder angle steering can be quantified. Considering that the calculation of the safety encounter distance involves a ship's navigation safety, a relatively conservative 10° rudder angle can be applied to calculate the ship's directional keeping capacity.

The traditional calculation methods for the transverse force of the rudder on the hull and the moment of the turning bow on the hull are presented as

$$\begin{cases} X_R = (1 - t_R) F_N \sin\delta \\ Y_R = (1 + a_H) F_N \cos\delta \\ N_R = (x_R + a_H x_H) F_N \cos\delta \end{cases} \tag{9}$$

where t_R = coefficient of rudder drag derating, a_H = increment coefficient of the rudder, x_R = coordinate value of the action centre of the rudder force, x_H = centre coordinate value of the action of fluid force caused by steering, δ = rudder angle and F_N = positive pressure of the rudder, which can be expressed as

$$F_N = -0{\cdot}5\rho A_R f_\alpha U_R^2 \sin\alpha_R \tag{10}$$

where A_R = area of the rudder, f_α = coefficient of normal force, U_R = effective velocity at the rudder and α_R = effective angle of attack at the rudder. Therefore, the transverse force of the rudder on the hull and the moment of the turning bow on the hull can be implicitly expressed as

$$\begin{cases} Y_R = f(a_H, A_R, f_\alpha, U_R, \alpha_R, \delta) \\ N_R = f(a_H, x_H, A_R, f_\alpha, U_R, \alpha_R, \delta) \end{cases} \tag{11}$$

According to Equation (11), the parameters for calculating the transverse force of the rudder on the hull and the moment of the turning bow on the hull can be obtained. Although these parameters can be

https://doi.org/10.1017/S037346332000065X Published online by Cambridge University Press

obtained by empirical formulas, obtaining the parameters needed by the empirical formulas is difficult in the actual monitoring process. Therefore, it is necessary to calculate the values of the force and moment in another way. In the mathematical model of ship motion, the linear simplified formula of the ship's return angle velocity can be expressed as

$$r = \frac{(0{\cdot}5LY_v + N_v)Y_\delta \delta}{-Y_v(mx_G u - N_r) + N_v(mu - Y_r)} \tag{12}$$

where Y_v, Y_r, N_r, and N_v are derivatives of the ship linear hydrodynamics (Inoue et al., 1981), which can be expressed as

$$\begin{cases} Y_v = -0{\cdot}5\pi\rho d_m^2 U\left(1{\cdot}69 + 0{\cdot}08\dfrac{C_b B}{\pi d_m}\right) \\ Y_r = -0{\cdot}5\pi\rho d_m^2 LU\left(-0{\cdot}645 + 0{\cdot}38\dfrac{C_b B}{\pi d_m}\right) \\ N_v = -0{\cdot}5\pi\rho d_m^2 LU\left(0{\cdot}64 - 0{\cdot}004\dfrac{C_b B}{\pi d_m}\right) \\ N_r = -0{\cdot}5\pi\rho L^2 d_m^2 U\left(0{\cdot}47 - 0{\cdot}18\dfrac{C_b B}{\pi d_m}\right) \end{cases} \tag{13}$$

where x_G = coordinate value of a ship's centre of gravity, m = ship quality, and u = longitudinal component of the ship speed.

The first-order manoeuvrability equation of a ship is expressed as

$$r = K\delta \tag{14}$$

where K = ship manoeuvrability index. The calculation formula of the rudder force and moment can be obtained by combining Equations (12)–(14), which can be expressed as

$$\begin{cases} Y_R = \dfrac{K\delta(-Y_v(mx_G u - N_r) + N_v(mu - Y_r))}{0{\cdot}5LY_v + N_v} \\ N_R = \dfrac{0{\cdot}5LK\delta(-Y_v(mx_G u - N_r) + N_v(mu - Y_r))}{0{\cdot}5LY_v + N_v} \end{cases} \tag{15}$$

Convert Equation (15) to an implicit formula, which can be expressed as

$$\begin{cases} Y_R = f(L, m, d_m, V, x_G, K, \delta) \\ N_R = f(L, m, d_m, V, x_G, K, \delta) \end{cases} \tag{16}$$

Obtaining the parameters of Equation (16) is easier than those required in Equation (11), and the method of obtaining parameters will be introduced in Section 2.5.3.

3.2.3. Calculation of transverse safety distance

When two ships pass each other in a channel in a head-on situation or overtaking situation, the analysis of the forces on each ship in both cases is performed without temporarily considering other environmental factors, which can be expressed as follows:

Via a force and moment analysis of two ships in an encounter situation, it can be seen that the two ships will not only be affected by the moment of the turning bow but also form a transverse drift due to the transverse force in the encounter process. Therefore, the calculation of the transverse safety distance is divided into two parts: ship safety transverse encounter distance obtained from the moment balance and correction of the safety encounter transverse distance obtained from the force balance.

https://doi.org/10.1017/S037346332000065X Published online by Cambridge University Press

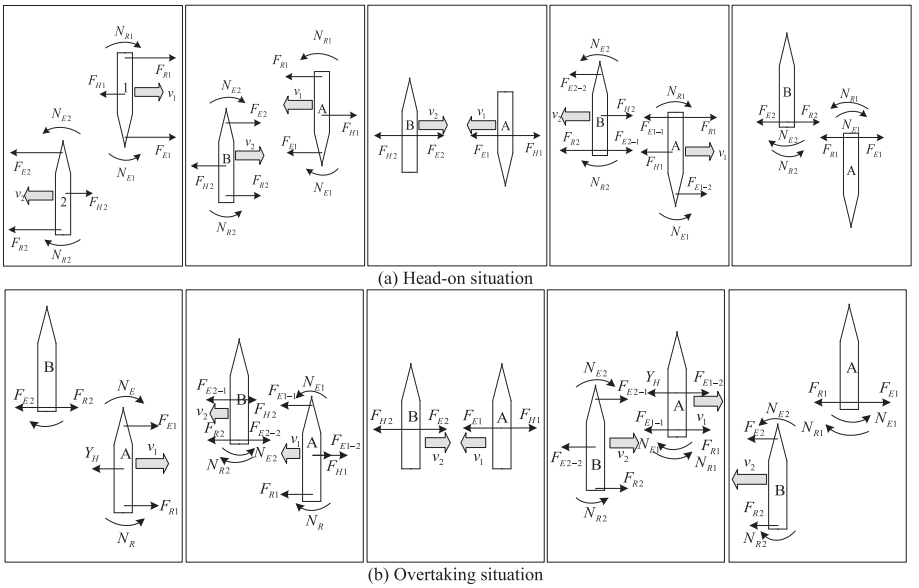

Figure 2. *Schematic of force and moment analysis in the condition of ship steerage: (a) Head-on situation; (b) Overtaking situation.*

To achieve the navigation safety of two ships in an encounter situation, both ships must satisfy the moment balance equation when the rudder angle is below the specified rudder angle δ_{max}. The expression is presented as

$$\begin{cases} f_{NE}(t_i, A(t), S_{P1}, U_1, U_2) \le f_{NRY}(L_1, m_1, d_{m1}, U_1, x_{G1}, K_1, \delta_{max}) \\ f_{NE}(t_i, A(t), S_{P2}, U_2, U_1) \le f_{NRY}(L_2, m_2, d_{m2}, U_2, x_{G2}, K_2, \delta_{max}) \end{cases} \tag{17}$$

Convert Equation (8) to an implicit expression. f_{NE}. is a function symbol of Equation (8). f_{NRY} is a function symbol of the rudder moment expression. When the rudder angle δ_{max} is limited, the maximum moment, which the rudder can produce is a fixed value. Therefore, the maximum value N_{Emax} and corresponding position t_{max} can be obtained. Equation (17) can be converted to:

$$\begin{cases} f_{NE}(t_i, A(t), S_{P1}, U_1, U_2) = f_{NRY}(L_1, m_1, d_{m1}, U_1, x_{G1}, K_1, \delta_{max}) \\ f_{NE}(t_i, A(t), S_{P2}, U_2, U_1) = f_{NRY}(L_2, m_2, d_{m2}, U_2, x_{G2}, K_2, \delta_{max}) \end{cases} \tag{18}$$

By solving Equation (18), the shortest transverse distance (S_{P1},S_{P2}), which two ships need to keep relative to the other ship, can be obtained. To ensure that neither ship turns its bow, the initial solution of the safety encounter transverse distance is taken as

$$S_{P0} = MAX(S_{P1}, S_{P2}) \tag{19}$$

It can be seen from the force analysis in Figure 1 that both ships have transverse drift in a head-on situation, overtaking situation and overtaken situation. The speed direction is different in different stages. Therefore, it is necessary to qualitatively analyse the direction of the ship drift. Use variable τ to express the drift condition:

$$\begin{cases} 1 & \text{away from other ship} \\ 0 & \text{without drift} \\ -1 & \text{close to other ship} \end{cases} \tag{20}$$

The qualitative analysis of the ship drift in both situations is shown in Figure 2.

https://doi.org/10.1017/S037346332000065X Published online by Cambridge University Press

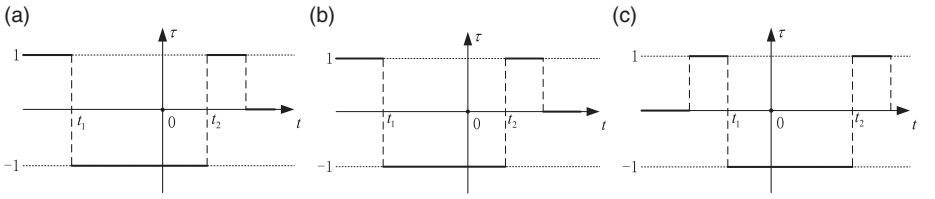

Figure 3. *Schematic of qualitative analysis of ship drift: (a) Head-on situation; (b) Overtaking situation; (c) Overtaken situation.*

According to the qualitative analysis results (shown in Figure 3), when two ships encounter each other in parallel and within a short distance, each ship begins to drift to the other ship when the nondimensional stagger distance is nearly 0. Assume that the initial solution of the safety encounter transverse distance S_{P0} is adopted as the transverse distance between the two ships. In the process of encountering, the transverse distance between the two ships will be less than S_{P0}. So that ships cannot satisfy the moment balance conditions, the bow will turn, which produces collision risk. Therefore, it is necessary to quantify the ship's transverse drift and determine its transverse drift distance ΔS_P. The time period is $[h_1, h_2]$., when the value of τ is -1. The amount of ship transverse drift during this period can be expressed as

$$\Delta S_P = \int_{h_1}^{h_2} v(h)dh \tag{21}$$

where v(h) = ship's transverse drift velocity at time h. According to the force balance principle, the ships satisfy the following requirement:

$$Y_R + Y_H + Y_E = 0 \tag{22}$$

Convert Equation (22) to an implicit form as

$$\begin{aligned} &f_{FRY}(L_1, m_1, d_{m1}, U_1, x_{G1}, K_1, \delta_{max}) + f_{FH}(v(h), Y_{v(h)}, Y_{r(h)}, Y_{vv(h)}, Y_{vr(h)}, Y_{rr(h)}) \\ &\quad + f_{FE}(t, S_P, U_1, U_2, H, d_m, L_1, L_2) = 0 \end{aligned} \tag{23}$$

The transverse drift velocity v(h) at time h can be obtained by solving the equation shown in Equation (23).

3.3. Longitudinal safety distance determination method

The longitudinal safety distance shall consider the avoidance ability of other ships, especially the restricted manoeuvrability of a ship, which does not have the ability and responsibility to avoid a collision with an overtaking ship or head-on ship. Therefore, the calculation of the longitudinal safety distance is mainly determined by the manoeuvrability of the other ship.

3.3.1. Ship manoeuvrability

The first-order ship manoeuvrability indices K and T proposed by Nomoto (Nomoto et al., 1957) can effectively describe the ship manoeuvrability, which can be expressed as

$$T\dot{r} + r = K\delta \tag{24}$$

where r = angular speed of the bow rotation and δ = angle of rudder. The instantaneous angular velocity, which disregards the time of the steering rudder can be expressed as

$$r = K\delta(1 - e^{-t/T}) \tag{25}$$

https://doi.org/10.1017/S037346332000065X Published online by Cambridge University Press

Assuming that the initial course angle is 0°, the course angle at any time can be obtained by the integral of Equation (23), which is shown as

$$\psi(t) = \psi_0 + K\delta(t - T + Te^{-t/T}) \tag{26}$$

The avoidance manoeuvring process of the overtaking ship is shown as Figure 4(a) and 4(b). The avoidance manoeuvring process of a head-on ship is shown in Figure 4(c) and 4(d).

The rudder angle determines the steering extent of a ship. When a smaller angle is utilised, more space is needed to avoid an overtaken ship so two ships can pass by with a safe transverse distance, as shown in Figure 2(b).

3.3.2. Longitudinal safety distance

Assuming that an overtaking ship is coming from the rear of the overtaken ship and disregarding the change in the ship speed, the relationship between the transverse safety distance and the longitudinal safety distance is expressed as

$$d_H = \int_0^{t_e} V \sin(\psi(t))dt \tag{27}$$

$$d_Z = \int_0^{t_e} V \cos(\psi(t))dt \tag{28}$$

The transverse safety distance (d_H) has been determined by the ship–ship effect calculation model and the ship's directional keeping capacity calculation model, as expressed in Equations (18)–(23). Therefore, the time of the overtaking process (t_e) is available. The longitudinal safety distance can be calculated by Equation (28). To give a certain manoeuvring allowance for overtaking a ship when the threat of overtaking a ship to the overtaken ship is detected. A smaller rudder angle, such as 10°, can be applied to estimate the longitudinal safe distance. Similarly, different rudder angles can be employed to estimate multiple longitudinal safety distances to establish different levels of alarm. When the overtaking ship is detected to be at risk to the overtaken ship, different alerts or warnings can be sent according to its risk level. A schematic of different levels of the ship domain are shown in Figure 5.

3.4. Estimation of related parameters

3.4.1. Analysis of parameter requirement

The novel ship domain model employed the ship–ship effect calculation model, ship's directional keeping capacity calculation model and ship manoeuvrability calculation model. However, the calculation models require part of the ship design parameters and ship navigation parameters. Combining the ship communication equipment and ship navigation equipment, it can be determined that the Automatic Identification System (AIS) is an effective way to obtain these parameters. The parameters provided by the AIS and the parameter requirement for calculation are shown in Figure 6.

According to Figure 6, the parameters of the marked shadows are not available from the AIS, and ρ and H are environmental parameters that can be easily obtained. K and T are the ship manoeuvrability indices. Therefore, the parameters provided by the AIS do not satisfy the application of the ship domain model, and the unavailable parameters need to be estimated.

3.4.2. Estimation of ship manoeuvrability

The estimation of the ship manoeuvrability indices employed the regression model proposed by Zhang (Zhang and Li, 2009). The regression models are expressed as

$$K' = 47{\cdot}875 - 2{\cdot}64\frac{L}{B} + 0{\cdot}004\frac{Ld_m}{A_R} + 66{\cdot}589C_b^2 - 112{\cdot}702C_b + 3{\cdot}826C_b\frac{L}{B} - 0{\cdot}293C_b\frac{B}{d_m} \tag{29}$$

https://doi.org/10.1017/S037346332000065X Published online by Cambridge University Press

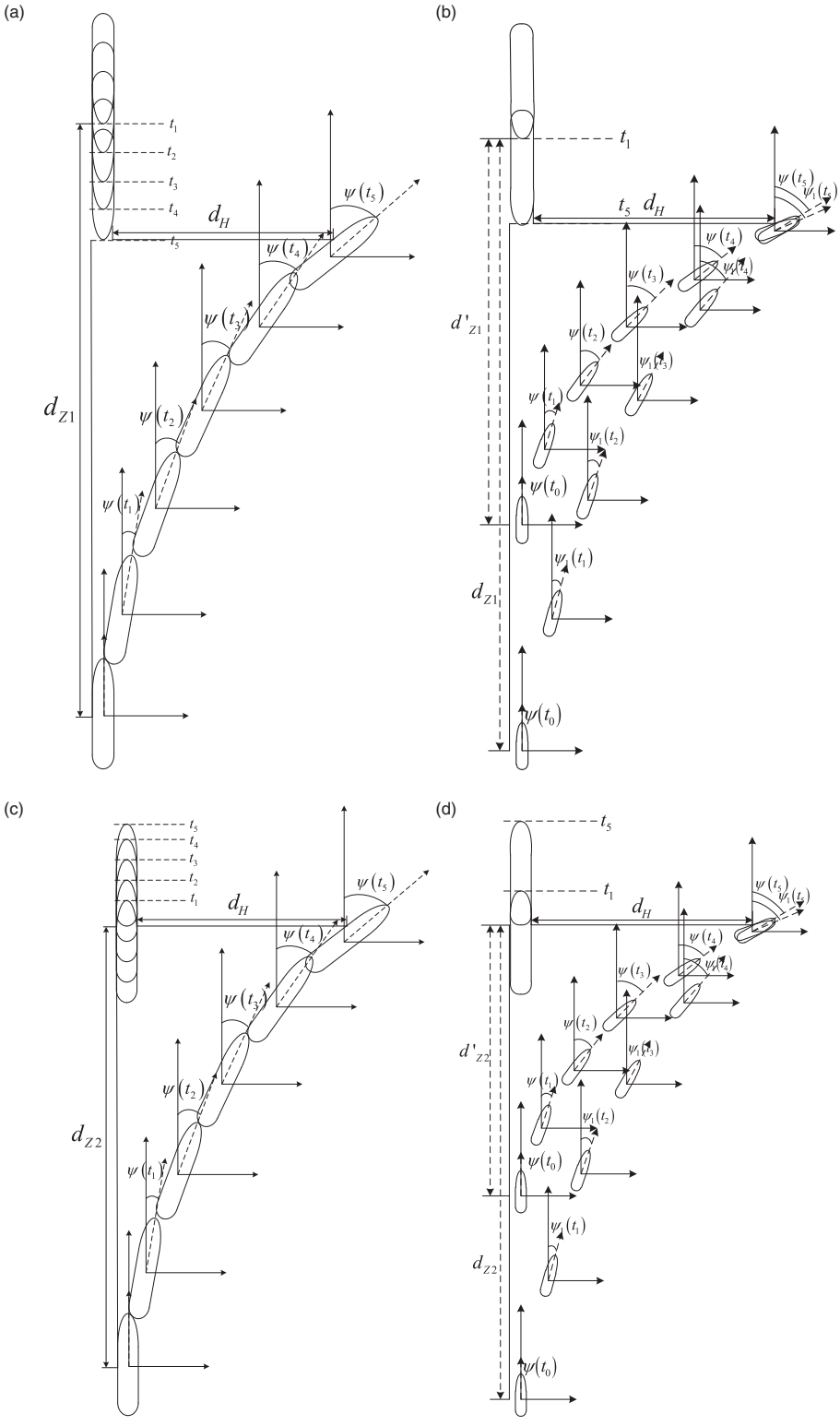

Figure 4. *Schematic of avoidance manoeuvring.*

https://doi.org/10.1017/S037346332000065X Published online by Cambridge University Press

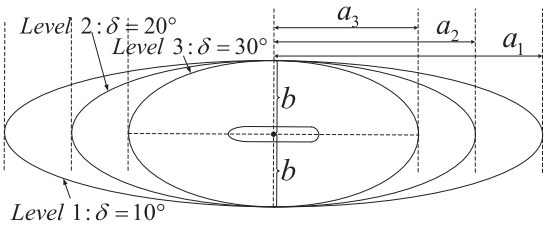

Figure 5. *Schematic of different levels of ship domain.*

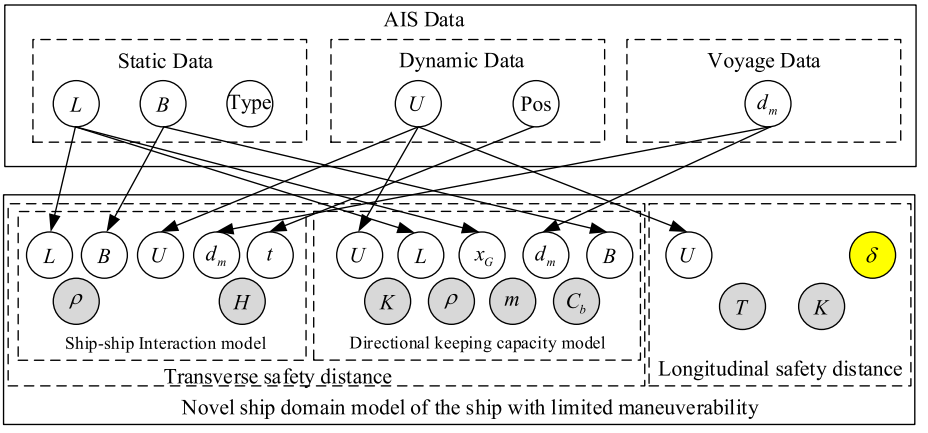

Figure 6. *Schematic of parameter supply and demand before estimation.*

$$T' = 26{\cdot}464 + 0{\cdot}408C_b\frac{Ld_m}{A_R} - 0{\cdot}033\frac{L^2d_m}{BA_R} - 79{\cdot}114C_b + 0{\cdot}757\frac{L}{B} + 46{\cdot}129C_b^2 \tag{30}$$

where C_b = square coefficient of the ship, A_R = size of the rudder, and K' and T' = nondimensional ship manoeuvrability indices. The dimensionalised formulas of the ship manoeuvring indices are expressed as

$$\begin{cases} K = K'\dfrac{v_s}{L} \\ T = T'\dfrac{L}{v_s} \end{cases} \tag{31}$$

The rudder response speed directly determines the collision avoidance effect when taking a turning measure to avoid a collision. The value of T represents the ability to follow the rudder angle. Therefore, underestimating the value of T can obtain the scale of the ship domain in a conservative way for the condition that the actual rudder response capability is unknown. To ensure the effectiveness of ship monitoring, avoid overestimating the ship's manoeuvring ability, which leads to the failure to remind a ship to conduct collision avoidance manoeuvring in time. The estimation of ship manoeuvrability needs part of the ship's design parameters. According to Figure 6, the uncertainty parameters of Equations (29) and (30) are v_s, C_b and A_R.

3.4.3. Estimation of ship design parameters

The Ship Information Database (SI-DB) can be established with part of the real ship data. When a ship's service speed v_s needs to be acquired, the ship's AIS data is utilised for extraction by the SI-DB. The parameters provided by the AIS and parameters provided by the SI-DB are shown in Figure 7.

When the parameters of the ship need to be expanded, obtain the MMSI of the ship from the AIS equipment. First, search the MMSI in the SI-DB; other parameters can be extracted directly if the MMSI

https://doi.org/10.1017/S037346332000065X Published online by Cambridge University Press

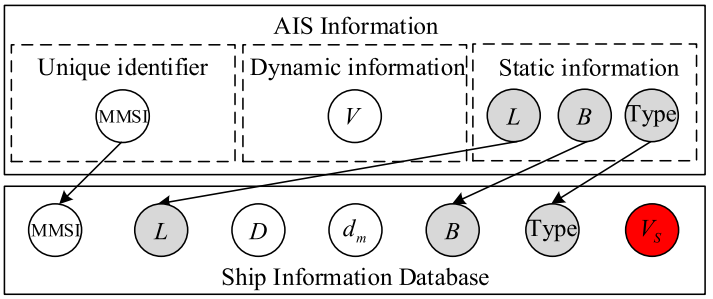

Figure 7. *Schematic of supply–demand relationship of parameters between AIS and Ship Information Database.*

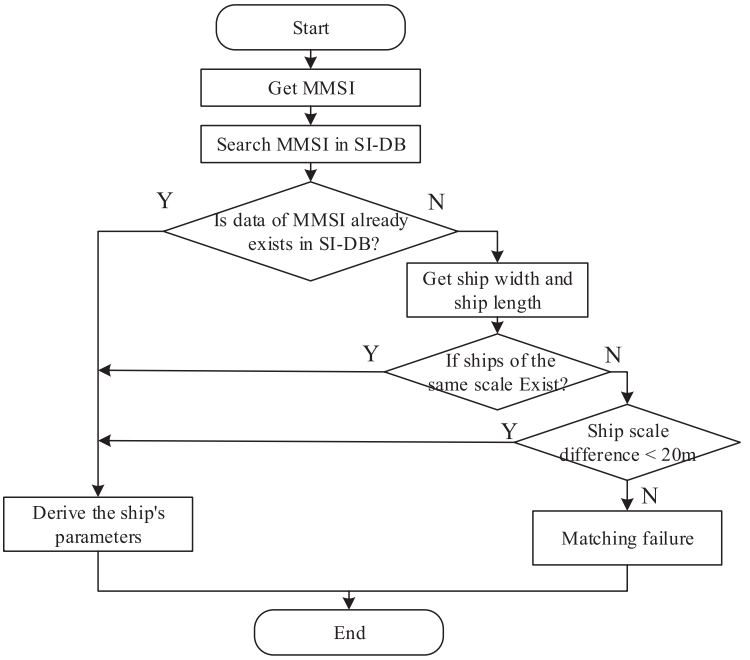

Figure 8. *Flow chart of ship database matching.*

exists. If the MMSI does not exist, obtain B_0, L_0 and type, calculate the Euclidean distance between the selected ship's parameters and the parameters of each ship with the same type applied in the SI-DB. Consider the parameters of a ship from the SI-DB with the shortest Euclidean distance as matching parameters. The calculation of the Euclidean distance is shown as

$$d(S_0, S_i) = \sqrt{(L_i - L_0)^2 + (B_i - B_0)^2} \tag{32}$$

The matching process in the SI-DB is shown in Figure 8.

C_b can be estimated by a regression formula, which regressed the real ship data. Katsoulis proposed a regression formula for bulk cargo ships, which is expressed as (Katsoulis, 1975)

$$C_b = 0{\cdot}8217 L^{0{\cdot}42} B^{-0{\cdot}3072} d_m^{0{\cdot}1721} V_s^{-0{\cdot}613} \tag{33}$$

However, the residual value of the Katsoulis formula is too large, as the data applied in the regression formula is too old, and the other types of ships do not have an existing regression formula. Therefore, the

https://doi.org/10.1017/S037346332000065X Published online by Cambridge University Press

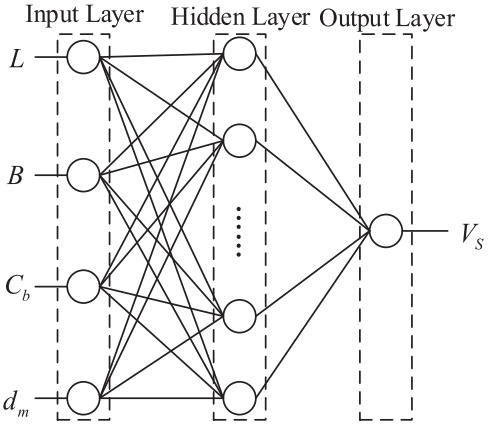

Figure 9. *Schematic of BP neural network structure.*

Table 1. *Normalised range of training parameters.*

Parameters	x_{top}	x_{bottom}
L (m)	20	500
B (m)	5	80
$\boldsymbol{C_b}$	0·4	1·0
$\boldsymbol{d_m}$ (m)	2	40
$\boldsymbol{v_s}$ (kn)	2	40

novel formula can be regressed as the form of Equation (33) with new ship data provided in Appendix 1. The results of the regression are shown as

$$\begin{cases} C_b = 1{\cdot}7067L^{0{\cdot}1851}B^{-0{\cdot}0803}d_m^{0{\cdot}0155}V_s^{-0{\cdot}5536} & \text{Bulk cargo ship} \\ C_b = 0{\cdot}4585L^{0{\cdot}4683}B^{-0{\cdot}0631}d_m^{0{\cdot}0735}V_s^{-0{\cdot}689} & \text{Multipurpose cargo ship} \\ C_b = 0{\cdot}6483L^{0{\cdot}1219}B^{-0{\cdot}0438}d_m^{0{\cdot}0190}V_s^{-0{\cdot}1317} & \text{Tanker} \\ C_b = 0{\cdot}9237L^{0{\cdot}5606}B^{-0{\cdot}3021}d_m^{-0{\cdot}0085}V_s^{-0{\cdot}7573} & \text{Container ship} \end{cases} \tag{34}$$

The BP neural network is extensively applied in various fields due to its strong nonlinear mapping ability. Therefore, the BP neural network model can be employed to estimate the service speed of the ship. The model structure is shown in Figure 9.

According to the regression formula, the input layer neuron parameters of the BP neural network are set to L, B, C_b and d_m. The output layer neuron parameters are the service speed v_s, and the number of hidden layer neurons is nine, according to the method of the reference (Xiaorui and Changchuan, 2011). A sigmoid function is selected as the activation function

$$f(x) = \frac{1}{1 + e^{-x}} \tag{35}$$

The training parameters are normalised by Equation (33), where x_{top} and x_{bottom} are the maximum value and minimum value set for the parameters, considering the actual situation of ship development. The values are shown in Table 1.

https://doi.org/10.1017/S037346332000065X Published online by Cambridge University Press

Table 2. *Statistical results of rudder area for different ship types.*

Type	Value range of μ(%)	Selection value of μ(%)
Tanker	1·28–1·82	1·28/1·82
Bulk cargo ship	1·49–4·00	1·49/4·00
Container ship	2·41–3·85	2·41/3·85

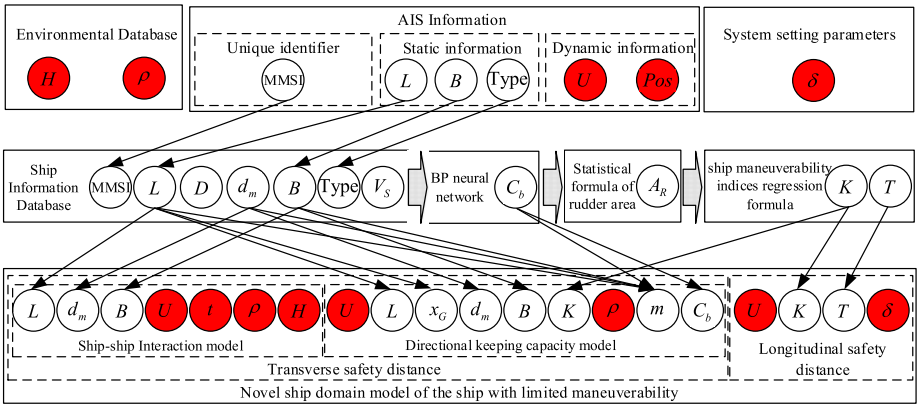

Figure 10. *Schematic of parameter supply and demand after estimation.*

The relationship between the ship mass m and the square coefficient C_b is shown as

$$C_b = \frac{m}{LBd_m} \tag{36}$$

The size of rudder (A_R) can be estimated with a large quantity of real ship data. The estimation formula can be expressed as

$$A_R = Ld_m\mu \tag{37}$$

The statistical results of μ and selection value of μ are shown in Table 2.

According to the analysis results of the selection principle of T. The selection value of μ can be determined as

$$\begin{cases} \left(0{\cdot}408C_b - 0{\cdot}033\dfrac{L}{B}\right) > 0 \ \text{Select higher value} \\ \left(0{\cdot}408C_b - 0{\cdot}033\dfrac{L}{B}\right) < 0 \ \text{Select lower value} \end{cases} \tag{38}$$

3.4.4. Result of model parameters supply and requirement

The estimation method of unavailable parameters is established. The novel ship domain model can be realised in the monitoring system, which acquires ship data by the AIS signal. The relationship of the parameters supply and parameters requirement between the AIS and the ship domain model is shown in Figure 10.

The parameters with a red shadow are mainly divided into three categories: Parameters directly obtained via the AIS, parameters set by the system, and environmental parameters, which can be applied directly without any other operation.

https://doi.org/10.1017/S037346332000065X Published online by Cambridge University Press

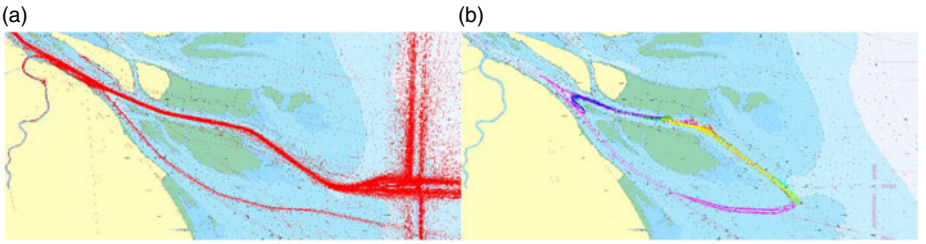

Figure 11. *Ship distribution in North Channel: (a) AIS data of ships in North Channel; (b) AIS data of dredgers in North Channel.*

Table 3. *Parameters of the self-propelled trailing-suction hopper dredger.*

Parameter	Value
Length (m)	165·00
Width (m)	27·00
Draught (m)	7·10
Service speed (kn)	15
Dredging speed (kn)	3

4. Experiment and analysis

4.1. Data of experimental ship

To detect the validity of the proposed ship domain model, a reasonable water area and ship data need to be selected. The length of the channel of the North Channel of the Yangtze River Estuary is approximately 43 nautical miles. The width of the channel extends from 350 m to 400 m. The depth at the lowest tide is 12·5 metres. Therefore, the North Channel is the most important channel to enter the Yangtze River Channel, which can satisfy the draught requirements of large ships compared with the channel of South Channel. Moreover, due to the natural factors of Yangtze River Basin, dredgers carry out dredging work in the channel for a long time to maintain the depth of the channel. The North Channel not only has a high density of ship traffic flow [shown in Figure 11(a)] but also is accompanied by the dredging work of the trailing suction dredger [shown in Figure 11(b)]. Therefore, the novel ship domain model can be detected with the ship traffic flow data in the North Channel of the Yangtze River Estuary.

Several dredgers are working in the North Channel. A self-propelled trailing suction hopper dredger is a typical ship with restricted manoeuvrability during operation. Therefore, a self-propelled trailing suction hopper dredger can be employed to detect the proposed ship domain model. Part of the parameters of the self-propelled trailing suction hopper dredger is shown in Table 3.

4.2. Comparison of different models

Different ship domain models have different boundaries. To show the advantage of the proposed ship domain model for ships with restricted manoeuvrability in busy waters, several classical ship domain models are employed for calculation with the parameters of Table 3. The boundaries of these models are shown in Figure 12.

The boundary determination method is presented in the references (Fujii and Tanaka, 1971; Goodwin, 1975; Davis et al., 1980; Coldwell, 1983; Hansen et al., 2013). The ship domain model proposed by Davis is based on the Goodwin model. The size of the Davis model is the same as the size of the Goodwin model, which are both too large to be applied to busy waters. Therefore, the Goodwin model is employed

https://doi.org/10.1017/S037346332000065X Published online by Cambridge University Press

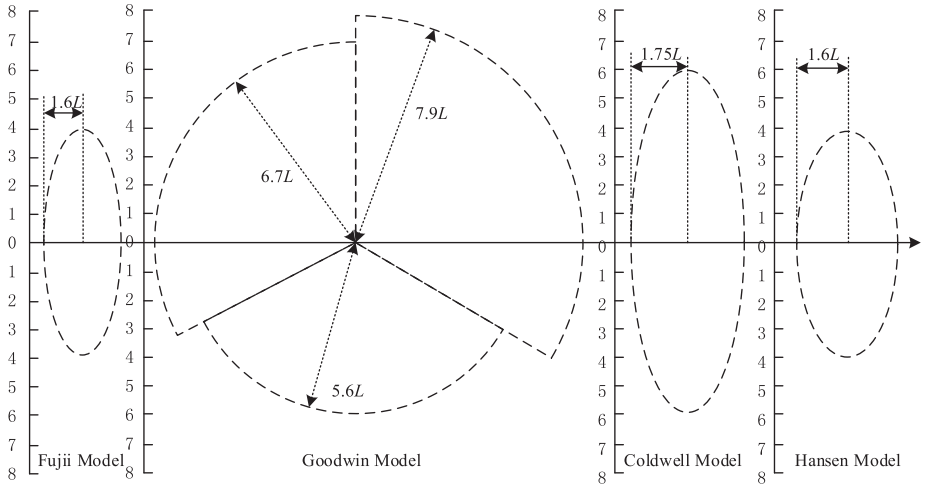

Figure 12. *Boundaries of four classical ship domain models.*

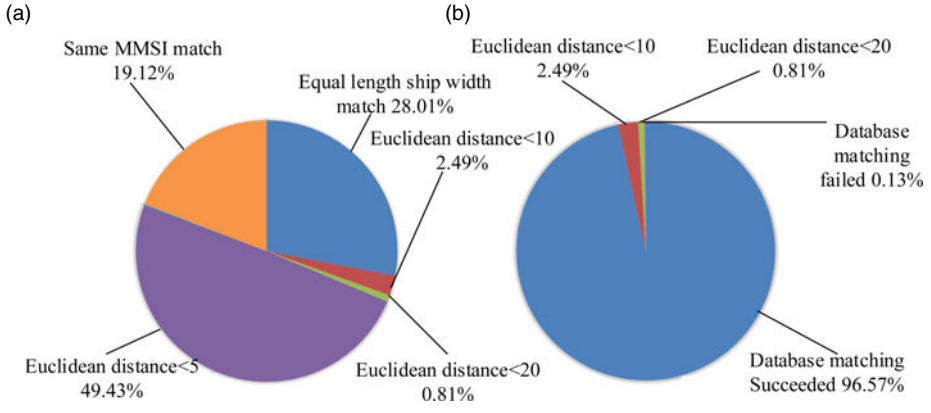

Figure 13. *Matching results of measured AIS data in Shanghai North Channel.*

as a reference, and the Fujii model, Coldwell model and Hansen model can be utilised to detect the collision risk of ships in busy waters to compare the advantages of the novel ship domain model.

4.3. Analysis of ship parameter estimation results

4.3.1. Performance analysis of ship parameters database

The method of parameter estimation is employed to expand the ship parameters. The accuracy of estimation formulas for the rudder area and ship manoeuvrability index are not verified as they have been certified by relevant scholars. In this paper, the SI-DB is proposed to expand the ship parameters. The parameter expansion experiment is carried out with AIS data (oil tanker, container ship and dry bulk carrier) of the North Channel of the Yangtze River Estuary. The matching results are shown in Figure 13.

The probability of the Euclidean distance below 5 m (including successful matching) is approximately 96·57%. According to the selection principle of ship construction parameters, ships have similar dimensions, and the same type of ship should have a similar navigation performance. Thus, 95·57% of ships can carry out reasonable parameters expansion when matching parameters with the SI-DB [as shown in Equation 5(b)]. It is reasonable to carry out follow-up calculation.

https://doi.org/10.1017/S037346332000065X Published online by Cambridge University Press

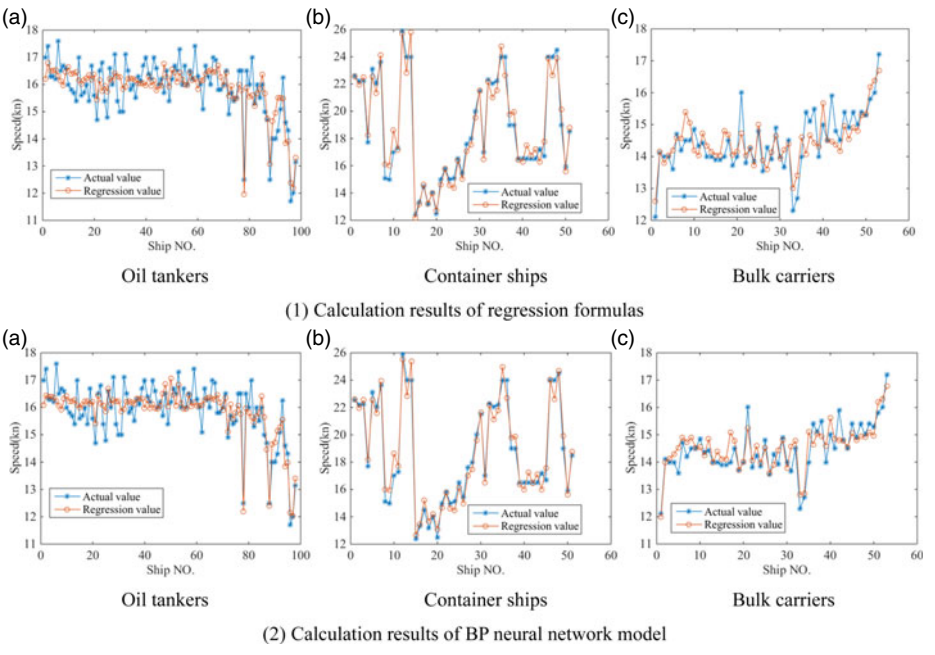

Figure 14. *Comparison of experimental results: (1) Calculation results of regression formulas (a) Oil tankers (b) Container ships(c) Bulk carriers; (2) Calculation results of BP neural network model (a) Oil tankers (b) Container ships (c) Bulk carriers.*

Table 4. *Comparison of statistical remainder values.*

	Average value (%)		Variance		Maximum value (%)	
Type	Regression formulas	BP neural network model	Regression formulas	BP neural network model	Regression formulas	BP neural network model
Oil tankers	3·3435	3·0398	4·7285	4·2758	8·5079	8·2098
Container ships	2·9579	3·1458	5·2448	4·1911	9·5595	9·0925
Bulk carriers	2·8228	2·4144	4·8923	4·0750	8·9916	7·9333

4.3.2. Performance analysis of BP neural network model

The equations obtained by multiple nonlinear regression are compared with the calculation results of the BP neural network model. The data of 53 bulk carriers, 51 container ships and 98 oil tankers are employed for calculation. The calculation results are shown in Figure 14.

The residual results of the two methods are counted and shown in Table 4.

The results calculated by the BP neural network model, which is trained by actual ship data, are compared with the results calculated by a regression formula. The average residuals of the two methods are less than 5%, which means that the two methods can be effective methods for estimating ships' service speeds. To further compare the estimation performance of the two methods, the variation in the residual statistical results of the two methods are shown in Table 5.

4.4. Calculation and comparison

The parameters provided in Table 3 can be utilised to compute the novel ship domain model in the North Channel of Yangtze River Estuary. Real AIS data of past ships during dredging construction are

https://doi.org/10.1017/S037346332000065X Published online by Cambridge University Press

Table 5. *Advantage of BP neural network computing model compared with regression formula.*

Type	Reduction of average value (%)	Reduction of variance (%)	Reduction of maximum value (%)
Oil tankers	9·0833	9·5739	3·5038
Container ships	−6·3525	20·0904	4·8852
Bulk carriers	14·4679	16·7058	11·7699

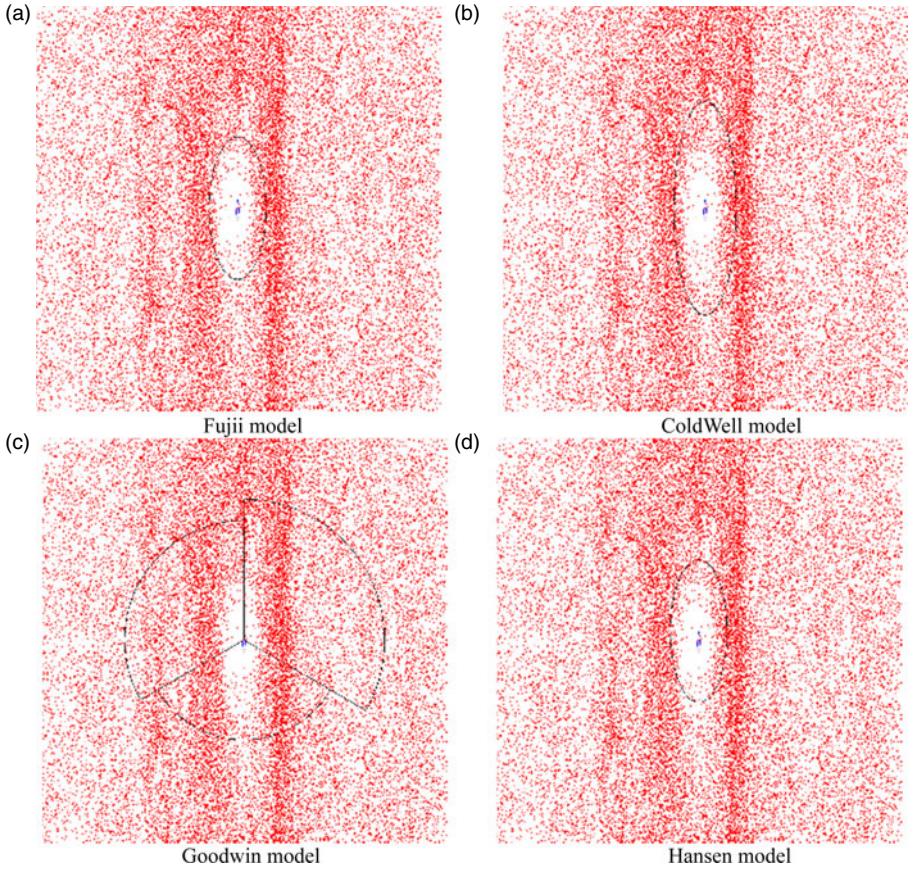

Figure 15. *Calculation results of ship domain models: (a) Fujii model; (b) ColdWell model; (c) Goodwin model; (d) Hansen model.*

employed to detect the advantages and effectiveness of the ship domain model. Simultaneously, the Fujii model, Coldwell model, Goodwin model and Hansen model are applied to the prediction of collision risk for a comparison.

AIS data are gradually sent to the model according to the order of real reception. The standard of risk detection is described as follows: If another ship's position is inside the boundary of the dredger ship domain, the risk of collision is assumed, which warrants a warning. Subsequent operations are not the research content of this paper.

The experimental records are shown in Figure 15.

The experimental data recorded during the experiment, as shown in Table 6, are employed for quantitative comparison.

https://doi.org/10.1017/S037346332000065X Published online by Cambridge University Press

Table 6. *Values to be recorded and calculated in experiment.*

Variable	Variable meaning
$\boldsymbol{P_t}$	Number of AIS data points of the ship that encounters dredger
$\boldsymbol{P_I}$	Number of AIS points inside the boundary of ship domain
$\boldsymbol{S_t}$	Number of ships that encounter dredger
$\boldsymbol{S_I}$	Number of ships that have ever been inside the boundary of ship domain
$\boldsymbol{\xi_P}$	Point alarm rate: $\xi_P = P_I/P_t$
$\boldsymbol{\xi_S}$	Ship alarm rate: $\xi_S = S_I/S_t$

Table 7. *Statistical results of four ship domain models and novel ship domain.*

Model	Fujii	ColdWell	Goodwin	Hansen	Proposed ship Domain (Level 1)	Proposed ship Domain (Level 2)	Proposed ship domain (Level 3)
$\boldsymbol{P_t}$	79871	79871	79871	79871	79871	79871	79871
$\boldsymbol{P_I}$	1984	4503	27752	1948	964	488	15
$\boldsymbol{\xi_P}$ (%)	2·484	5·638	34·746	2·439	1·207	0·611	0·019
$\boldsymbol{S_t}$	3483	3483	3483	3483	3483	3483	3483
$\boldsymbol{S_I}$	372	634	2050	372	107	45	2
$\boldsymbol{\xi_S}$ (%)	10·680	18·203	58·857	10·680	3·072	1·292	0·057

The meaning of the point alarm rate $\boldsymbol{\xi_P}$ is shown in Table 6. Its calculation meaning is that when a new AIS data message is obtained by the system. First, the message must be decoded and information, such as a ship's position, must be generated. Collision risk testing will be carried out by the ship domain model. If risk exists, an alarm prompt will be generated. Therefore, the point alarm rate can reflect the actual response frequency of the system. The significance of the ship alarm rate $\boldsymbol{\xi_S}$ is more direct. Based on the point alarm rate, part of the continuous alarms will be recognised from the same ship via data matching, which can truly reflect the sensitivity of the model for ship collision risk identification. If the value of $\boldsymbol{\xi_S}$ is high, the ship domain model is overly sensitive, and the risk detection of the ships encountered is too strict to effectively identify ships with potential collision risks. Thus, a substantial number of collision risk alarms, which will increase the burden of staff, are generated. Therefore, when normal sailing ship data are employed in experiments, the lower are the values of $\boldsymbol{\xi_P}$, the better should be the values of $\boldsymbol{\xi_S}$.

The quantitatively comparison of the statistical results of each model is shown in Table 7.

It can be seen from Table 7 that, compared with other classical ship domain models, the proposed ship domain model utilised AIS data of normal navigation for detection. The Goodwin model has the highest false alarm rate, which is not applicable for risk identification in this case. Compared with the Goodwin model, the Fujii model, Coldwell model and Hansen model are smaller, and the alarm rate reduced to 10%–20%. However, when the Goodwin model is employed for normal navigable waters, the false alarm rate is still high, which will produce more frequent alarm information. The proposed ship domain model considers the parameters of both sides, which cause it to have different forms for different ships and different environments. Therefore, the false alarm rates of three levels of the novel ship domain model are reduced to 3·072%, 1·292% and 0·057%, respectively. However, the third level of the proposed ship domain model adopts the manoeuvring mode of ship emergency avoidance to avoid collision, which is rarely applied in the process of ship navigation. Using the third level of the ship domain model only will lead to the detection of the risk of two ships, which are already in a very

https://doi.org/10.1017/S037346332000065X Published online by Cambridge University Press

critical situation. Therefore, three-level detection can be employed to distinguish ships with different degrees of danger to own ship. The first level of the ship domain model can be utilised to preliminarily detect ships around one ship, which may cause collision risks. The other two levels of the ship domain model can divide these ships into two groups, which causes different degrees of risk to the ship. When the collision risk of other ships increases, the model can be focused on tracking and alerting. Compared with the four classical models, the false alarm rate of the first level of the novel ship domain model decreased by 7·608%, 15·131%, 55·785% and 7·608%. Therefore, the proposed ship domain model can effectively reduce the false alarm rate of the ship risk in busy waters.

5. Conclusion

The safety of ship navigation is always an important research issue in the navigation field. The navigation safety of ships with restricted manoeuvrability is directly related to the navigation safety of the channel in busy waters. In particular, most ships with limited manoeuvrability are engineering ships in operation. The collision accidents of these ships will cause not only great economic losses but also cause casualties and destroy engineering achievements. Therefore, the collision risk identification of ships with restricted manoeuvrability has significance in busy waters.

However, the boundary of the classical ship domain model is too large to effectively identify collision risks. The differences in the threat among different ships are not considered, which directly leads to the poor effect of risk identification. The emergence of these alarms hinders the ability of channel managers or pilots to effectively distinguish ships with a real collision threat. Therefore, this paper analyses the characteristics of ships with restricted manoeuvrability sailing in busy waters and discovered the more important factors that lead to the collision risk of two ships in the process of navigation. A novel ship domain model for ships with restricted manoeuvrability in busy waters that is combined with ship manoeuvrability is proposed.

By verification of AIS trajectory data, the proposed ship domain model experiences a significant decrease in the alarm rate when it is applied to a self-propelled trailing suction dredger in busy waters. This way enables extraction of a smaller part of the ships near the study ship from all the passing ships, which poses a greater threat to collision accidents.

Detection of ship collision risk is the primary step of ship collision avoidance. After confirming the ships with a high risk of ship collision, special tracking observation can effectively prevent ship collision. The navigation characteristics of different types of ships in different water areas and different working conditions are quite different. This paper conducted targeted research on engineering ships in operation. The equipment cost of an engineering ship is generally high, and engineering ships will suffer significant economic losses after a collision. From the perspective of water construction engineering, the damage to an engineering ship will greatly affect the progress of a project and indirectly cause a far-reaching impact.

Consequently, the proposed novel ship domain model can be effectively applied to ships with limited manoeuvrability in busy waters. For example, the self-propelled trailing suction dredger dredges in a narrow channel. Based on this paper, other types of ship domain models in a water area can be investigated. This paper presented a new form of analytical method in the study of ship domain models. This paper proposed a multi-level ship domain model that is based on the classical ship domain model. The purpose of the multi-level concept is to effectively observe the risk change trend of ships when ships enter the ship domain model. Compared with the classical ship domain model, the proposed ship domain model has a more three-dimensional monitoring effect. Based on the current research results, future studies will focus on the application of the ship domain model in busy waters and the construction of the ship domain model in other special waters.

Funding statement. This work was supported by the 'The National Key Research and Development Program of China' [2017YFC0805309], 'The Fundamental Research Funds for the Central Universities' [3132019303] and 'The Natural Science Foundation of Zhejiang Province' [LQ20G020011].

References

Argüelles, R. P., Maza, J. A. and Martín, F. M. (2019). Specification and design of safety functions for the prevention of ship-to-ship collisions on the high seas. *Journal of Navigation*, **72**(1), 53–68.

Coldwell, T. G. (1983). Marine traffic behaviour in restricted waters. *The Journal of Navigation*, **36**(3), 430–444.

Curtis, R. G. (1980). The probability of close overtaking in fog. *Journal of Navigation*, **33**(03), 329.

Davis, P. V., Dove, M. J. and Stockel, C. T. (1980). A computer simulation of marine traffic using domains and arenas. *Journal of Navigation*, **33**(02), 215.

Dinh, G. H. and Im, N. K. (2016). The combination of analytical and statistical method to define polygonal ship domain and reflect human experiences in estimating dangerous area. *International Journal of e-Navigation and Maritime Economy*, **4**, 97–108.

Fiskin, R., Nasiboglu, E. and Yardimci, M. O. (2020). A knowledge-based framework for two-dimensional (2D) asymmetrical polygonal ship domain. *Ocean Engineering*, **202**, 107187.

Fujii, Y. and Tanaka, K. (1971). Traffic capacity. *Journal of Navigation*, **24**(04), 543.

Goerlandt, F., Montewka, J., Zhang, W. and Kujala, P. (2016) An analysis of ship escort and convoy operations in ice conditions. *Safety Science*, **95**, 198–209.

Goodwin, E. M. (1975). A statistical study of ship domains. *The Journal of Navigation*, **28**(3), 17.

Gourlay, T. (2009). Sinkage and trim of two ships passing each other on parallel courses. *Ocean Engineering*, **36**(14), 1119–1127.

Hansen, M. G., Jensen, T. K., Lehn-SchiøLer, T., Melchild, K., Rasmussen, F. M. and Ennemark, F. (2013). Empirical ship domain based on AIS data. *Journal of Navigation*, **66**(06), 931–940.

Hörteborn, A., Ringsberg, J. W., Svanberg, M. and Holm, H. (2018). A revisit of the definition of the ship domain based on AIS analysis. *Journal of Navigation*, 1–18.

Im, N. and Luong, T. N. (2019). Potential risk ship domain as a danger criterion for realtime ship collision risk evaluation. *Ocean Engineering*, **194**, 106610.

Inoue, S., Hirano, M. and Kijima, K. (1981). Hydrodynamic derivatives on ship maneuvering. *International Shipbuilding Progress*, **28**(321), 112–125.

Jingsong, Z., Zhaolin, W. and Fengchen, W. (1993). Comments on ship domains. *Journal of Navigation*, **46**(03), 422.

Katsoulis, P. S. (1975). Optimizing block coefficient by an exponential formula. *Shipping World & Shipbuilder*, **168**, 217–219.

Lataire, E., Vantorre, M., Delefortrie, G. and Candries, M. (2012). Mathematical modelling of forces acting on ships during lightering operations. *Ocean Engineering*, **55**, 101–115.

Nomoto, K., Taguchi, T., Honda, K. and Hirano, S. (1957). On the steering qualities of ships. *International Shipbuilding Progress*, **4**(35), 354–370.

Pietrzykowski, Z. (2008). Ship's fuzzy domain – a criterion for navigational safety in narrow fairways. *Journal of Navigation*, **61**(3), 499–514.

Pietrzykowski, Z. and Uriasz, J. (2009). The ship domain – a criterion of navigational safety assessment in an open sea area. *Journal of Navigation*, **62**(01), 93.

Van der Tak, C. and Spaans, J. A. (1977). A model for calculating a maritime risk criterion number. *Journal of Navigation*, **30**(2), 287–295.

Varyani, K. S. and Krishnankutty, P. (2006). Modification of ship hydrodynamic interaction forces and moment by underwater ship geometry. *Ocean Engineering*, **33**(8), 1090–1104.

Varyani, K. S., Thavalingam, A. and Krishnankutty, P. (2004). New generic mathematical model to predict hydrodynamic interaction effects for overtaking maneuvers in simulators. *Journal of Marine Science & Technology*, **9**(1), 24–31.

Wang, N. (2010). An intelligent spatial collision risk based on the quaternion ship domain. *Journal of Navigation*, **63**(04), 733–749.

Wang, N. (2013). A novel analytical framework for dynamic quaternion ship domains. *Journal of Navigation*, **66**(02), 265–281.

Wang, Y. and Chin, H. C. (2016). An empirically-calibrated ship domain as a safety criterion for navigation in confined waters. *Journal of Navigation*, **69**(2), 257–276.

Wang, X., Liu, Z. and Cai, Y. (2017). The ship maneuverability based collision avoidance dynamic support system in close-quarters situation. *Ocean Engineering*, **146**, 486–497.

Xiaorui, H. and Changchuan, L. (2011). A preliminary study on targets association algorithm of radar and AIS using BP neural network. *Procedia Engineering*, **15**, 1441–1445.

Yeung, R. W. (1978). On the interactions of slender ships in shallow water. *Journal of Fluid Mechanics*, **85**(01), 143.

Zhang, X. K. and Li, Y. K. (2009). Prediction of Ship Maneuverability Indices. *Navigation of China*, **32**(1), 96–101.

Zhang, L. and Meng, Q. (2019). Probabilistic ship domain with applications to ship collision risk assessment. *Ocean Engineering*, **186**, 106130.

Zhang, W., Feng, X., Qi, Y., Shu, F. and Wang, Y. (2019). Towards a model of regional vessel near-miss collision risk assessment for open waters based on AIS data. *Journal of Navigation*, **72**(6), 1–20.

Zhao-Kun, W., Xin-Lian, X. and Wen-Bo, L. (2020). Self-adaption vessel traffic behaviour recognition algorithm based on multi-attribute trajectory characteristics. *Ocean Engineering*, **198**, 106995.

Zhou, D. and Zheng, Z. (2018). Dynamic fuzzy ship domain considering the factors of own ship and other ships. *Journal of Navigation*, **72**(2), 1–16.

Zhu, X., Xu, H. and Lin, J. (2001). Domain and its model based on neural networks. *Journal of Navigation*, **54**(1), 97–103.

Appendix

Data for regression formula

Bulk cargo ship									
L	*B*	*d*	C_b	V_s	*L*	*B*	*d*	C_b	V_s
89·960	14·50	6·400	0·804	12·1	192·60	28·00	14·360	0·541	15·0
109·95	17·40	7·930	0·783	12·3	192·80	31·50	11·500	0·792	14·8
123·95	17·40	8·000	0·810	12·7	199·80	30·20	11·700	0·762	16·0
145·00	27·20	4·240	0·701	16·0	199·90	32·26	13·300	0·873	13·8
155·00	27·20	9·880	0·740	15·4	199·99	32·26	12·500	0·845	14·0
164·00	22·00	9·500	0·739	14·0	215·40	37·00	12·800	0·819	14·5
175·00	31·00	5·600	0·750	15·8	225·00	32·26	14·200	0·861	13·6
176·20	26·00	10·06	0·834	14·1	229·00	32·26	14·620	0·864	14·9
179·90	30·00	10·00	0·840	14·0	235·00	38·00	14·500	0·869	13·7
179·90	30·00	10·60	0·854	14·0	249·88	43·00	15·000	0·829	14·7
179·90	28·40	10·90	0·759	15·5	250·00	43·00	13·990	0·823	14·0
179·95	32·00	10·50	0·808	14·0	270·00	44·00	17·520	0·827	14·9
179·95	32·00	10·50	0·791	14·3	284·20	45·60	16·520	0·827	15·4
180·00	30·00	10·65	0·834	13·8	288·90	45·00	17·620	0·839	15·0
182·80	22·40	10·53	0·775	15·1	289·00	44·00	17·960	0·817	15·4
183·00	31·50	5·160	0·747	17·2	291·80	45·00	18·250	0·846	14·4
184·10	31·00	10·72	0·797	14·0	292·00	45·00	18·400	0·857	14·9
189·00	31·20	10·70	0·787	14·5	299·50	50·00	18·400	0·863	14·5
189·10	32·00	10·70	0·790	15·9	300·00	49·00	18·600	0·881	14·2
189·90	32·26	11·20	0·847	13·9	312·00	47·50	18·040	0·808	15·4
189·90	32·26	11·20	0·847	13·9	327·80	50·00	19·170	0·811	15·3
189·99	32·26	12·85	0·863	14·3	330·00	57·00	18·700	0·805	14·5
189·99	30·50	11·82	0·805	14·5	360·00	65·00	23·000	0·838	14·8
190·00	32·26	12·54	0·839	14·0	362·00	65·00	23·000	0·833	14·5
Container ship									
L	*B*	*d*	C_b	V_s	*L*	*B*	*d*	C_b	V_s
73·450	13·50	3·540	0·710	12·4	171·00	28·40	10·90	0·636	17·3
74·500	12·80	4·510	0·670	13·3	178·00	25·80	8·900	0·590	21·5
81·500	15·45	4·860	0·600	14·5	178·00	28·40	11·20	0·745	16·5
81·800	15·70	4·950	0·660	13·2	186·00	28·40	11·00	0·734	16·5
86·000	15·45	5·790	0·650	14·3	189·00	28·40	5·750	0·644	19·3
96·300	16·50	5·540	0·660	15·3	192·00	30·05	10·40	0·587	22·2
99·000	18·50	6·500	0·740	12·5	193·10	30·80	10·00	0·600	22·1
106·50	18·20	8·000	0·630	15·8	201·20	28·40	9·500	0·784	17·3
114·00	20·50	6·500	0·700	15·1	205·70	28·90	9·700	0·610	22·3
114·00	20·50	4·390	0·651	15·9	224·00	32·30	11·00	0·699	19·3
115·50	18·00	6·520	0·650	16·5	224·50	32·20	11·00	0·694	19·3
117·00	21·40	7·700	0·690	15·3	231·00	32·20	12·00	0·625	22·6
117·20	20·00	6·570	0·690	15·5	239·60	32·20	12·50	0·660	22·2
123·00	20·50	6·500	0·660	15·1	259·20	32·20	11·50	0·680	24·3

Continued.

https://doi.org/10.1017/S037346332000065X Published online by Cambridge University Press

Container ship

L	*B*	*d*	C_b	V_s	*L*	*B*	*d*	C_b	V_s
126·00	21·40	7·660	0·662	15·3	259·90	32·20	10·70	0·683	24·3
147·90	23·25	8·500	0·632	17·7	260·00	37·30	12·50	0·647	22·2
148·00	25·00	8· 000	0·660	17·6	260·00	37·30	12·50	0·646	23·1
153·00	25·60	9·200	0·650	18·3	263·30	32·20	12·00	0·627	24·3
155·00	24·50	7·900	0·600	20·3	264·20	32·20	11·50	0·653	24·3
157·00	28·40	9·900	0·628	16·7	267·00	39·80	12·30	0·606	24·5
158·20	28·40	10·70	0·680	17·3	279·90	40·30	14·00	0·578	25·9
158·20	28·40	11·00	0·687	16·5	299·90	48·20	14·50	0·687	22·0
158·20	28·40	11·00	0·688	17·2	300·00	42·80	13·50	0·673	24·3
158·20	28·40	5·640	0·605	18·5	335·30	48·60	15·00	0·657	23·6
160·00	28·40	11·00	0·674	16·5	347·00	42·80	14·50	0·662	24·3
162·00	28·40	11·30	0·650	16·5					

Tanker

L	*B*	*d*	C_b	V_s	*L*	*B*	*d*	C_b	V_s
79·000	13·00	5·300	0·738	12·5	258·50	39·40	16·13	0·765	15·8
100·50	18·00	6·800	0·728	12·0	258·50	40·20	15·03	0·779	16·0
102·70	17·80	6·600	0·738	11·7	260·00	38·00	15·00	0·819	16·5
105·50	16·60	6·600	0·703	13·2	265·00	42·00	16·50	0·797	16·6
160·00	28·60	6·400	0·792	12·5	265·00	44·20	16·76	0·826	15·3
184·84	32·26	12·10	0·795	14·6	270·10	42·50	15·82	0·785	17·0
185·00	25·20	10·30	0·766	15·5	270·10	42·50	15·82	0·739	16·4
185·00	28·40	10·40	0·806	14·0	270·10	42·50	15·83	0·788	16·2
187·22	32·25	12·10	0·803	14·3	270·10	42·50	16·28	0·762	17·0
192·00	26·50	10·40	0·795	16·0	270·10	42·50	16·68	0·791	16·2
192·00	26·80	10·40	0·783	15·0	273·00	48·00	17·15	0·819	14·0
210·00	30·50	11·50	0·795	17·0	273·10	42·00	15·50	0·789	15·5
211·70	28·80	10·89	0·786	17·0	273·80	42·00	15·50	0·787	16·0
216·30	30·50	11·79	0·768	16·5	274·00	43·50	17·03	0·794	15·4
216·30	30·50	11·47	0·791	16·7	276·00	43·00	16·50	0·807	16·5
216·40	28·20	11·11	0·768	17·4	278·00	44·20	15·03	0·774	16·3
219·00	32·20	12·19	0·828	15·4	278·00	44·20	15·03	0·773	16·1
220·00	31·10	11·60	0·826	16·5	278·00	44·20	15·00	0·775	16·7
220·00	35·60	12·17	0·826	14·7	288·00	45·60	15·38	0·763	16·5
220·50	31·00	11·77	0·778	17·0	290·00	48·20	18·50	0·838	15·5
221·30	30·50	11·52	0·776	17·6	291·00	43·00	16·57	0·788	15·7
221·70	30·50	12·27	0·740	16·0	300·00	48·20	17·29	0·751	16·7
222·50	30·50	12·02	0·777	15·7	300·00	48·20	18·03	0·802	16·5
222·50	30·50	12·02	0·771	15·4	306·50	47·50	16·04	0·785	16·2
224·30	30·50	11·48	0·781	16·6	313·00	50·80	17·80	0·797	16·0
224·40	30·50	11·60	0·791	15·8	313·00	48·20	19·30	0·839	16·0
224·50	30·50	11·44	0·775	16·3	317·00	50·40	17·00	0·789	17·3
224·50	30·50	11·45	0·774	16·3	317·00	50·00	20·73	0·811	16·5
224·50	30·50	11·53	0·774	16·2	319·30	53·00	19·50	0·814	16·7
225·40	32·00	12·53	0·779	15·7	319·30	53·00	19·50	0·815	16·0
228·00	32·20	12·19	0·810	15·6	321·80	52·40	19·89	0·811	17·4

Continued.

https://doi.org/10.1017/S037346332000065X Published online by Cambridge University Press

Tanker

L	*B*	*d*	C_b	V_s	*L*	*B*	*d*	C_b	V_s
228·50	32·20	12·80	0·769	15·4	321·80	52·40	19·85	0·868	16·3
231·20	35·60	12·30	0·802	14·7	324·00	54·00	19·53	0·789	16·2
233·90	32·80	12·00	0·807	16·7	324·00	53·00	19·42	0·816	16·0
234·00	33·20	12·00	0·787	16·0	324·00	53·00	19·45	0·815	15·1
235·00	32·20	12·68	0·815	15·6	331·50	54·80	20·58	0·799	15·8
238·50	36·00	12·22	0·795	14·8	331·50	56·00	20·58	0·817	16·0
238·60	36·50	12·04	0·775	16·8	333·00	60·00	21·13	0·802	14·9
240·00	35·30	12·23	0·797	15·4	333·00	60·00	21·30	0·810	14·3
242·00	37·20	14·60	0·818	16·0	333·00	60·00	21·70	0·813	15·1
243·00	35·30	12·00	0·788	16·5	333·00	60·00	22·50	0·819	16·2
243·00	35·30	13·02	0·791	16·0	335·00	58·00	22·72	0·799	15·7
244·50	34·80	13·84	0·784	17·1	336·30	54·50	19·59	0·809	16·7
245·60	36·50	12·43	0·761	16·6	336·90	53·60	19·74	0·821	16·3
253·00	36·80	14·53	0·794	15·4	337·10	54·50	19·93	0·805	17·0
254·30	37·20	14·86	0·796	15·0	337·10	54·50	19·90	0·806	16·9
257·00	38·80	14·78	0·822	16·5	337·70	53·60	19·74	0·819	16·0
257·10	40·20	14·50	0·782	15·0	338·00	54·40	20·96	0·818	16·5
258·50	40·20	15·07	0·781	17·1	341·00	53·50	20·00	0·813	15·8

Cite this article: Pan W, Xie X-l, Bao T-t, Li M (2021). Ship domain model for ships with restricted manoeuvrability in busy waters. *The Journal of Navigation* **74**: 3, 673–697. https://doi.org/10.1017/S037346332000065X